CCFE
CULHAM CENTRE FOR FUSION ENERGY

UK Atomic Energy Authority

UKAEA-CCFE-PR(21)17

T. A. Berry, C. R. Nobs, A. Dubas, R. Worrall, T. Eade, J. Naish, L. W. Packer

Integration of fluid dynamics into activation calculations for fusion

Integration of fluid dynamics into activation calculations for fusion

T. A. Berry, C. R. Nobs, A. Dubas, R. Worrall, T. Eade, J. Naish, L. W. Packer

This is a preprint of a paper submitted for publication in Fusion Engineering and Design

Integration of fluid dynamics into activation calculations for fusion

T.A. Berry[a], C.R. Nobs[a], A. Dubas[a], R. Worrall[a], T. Eade[a], J. Naish[a], L.W. Packer[a]

[a] *United Kingdom Atomic Energy Authority, Culham Centre for Fusion Energy, Culham Science Centre, Abingdon, Oxon, OX14 3DB, United Kingdom*

The accurate modelling of the activation of flowing material in a fusion reactor, such as coolant water or lithium-lead breeder, has important safety and shielding implications. Two codes developed at CCFE which account for neutron flux variation have been investigated for the effects of incorporating computational fluid dynamics (CFD) and benchmarked against experimental data. With the inclusion of CFD, benchmarking discrepancies previously identified for ^{16}N water activation data have been clarified and both codes are found to be accurate, with a remaining activity underestimation as low as 10.4% depending on the approach. Precise paths calculated using CFD have been used in flowing lithium-lead activation analysis for the first time, with results suggesting that simplified linear paths give comparable results to detailed CFD paths, but low-detail CFD paths should be avoided. This work paves the way for an accurate and benchmarked set of fluid activation codes.

Keywords: neutronics, fluids, codes, safety, experiment, benchmarking

1. Introduction

The movement and activation of fluids around coolant and breeding circuits in a fusion reactor are an important radiological consideration because flowing material can carry radioactivity to safety-critical areas [1]. This includes gamma-ray emission from activated fluid and activated corrosion products, and secondary activation resulting from neutron emission, with implications for the safety of maintenance personnel and damage to electrical equipment [2]. It is therefore desirable to perform activation analyses which account for fluid motion in a multi-physics approach. Two codes have been developed by CCFE to more accurately simulate fluid activation:

(i) ActiFlow was developed to calculate the decay heat of lithium-lead in breeder blankets, using FISPACT-II [3] to calculate the activity and decay heat in voxels of a flux mesh tally for multiple isotopes simultaneously. The use of FISPACT-II for material activation means that many reactions can be evaluated, making ActiFlow well-suited to simulating complex and heavy materials. It has not previously been benchmarked for fluid activation.

(ii) GammaFlow uses calculated reaction rates in cells to track the concentration of target isotopes around a system. The code requires knowledge of the nuclear reactions and decay modes to be tracked, and requires defined fluid cells. It is therefore well-suited to simulating activated coolant water circuits where there are few reactions of interest. It has been benchmarked previously [4].

In previous work [4] GammaFlow has been applied to the results of a 2019 ITER experiment at the Frascati Neutron Generator (FNG) investigating water activation phenomena associated with ^{16,17}N production, decay and transport [5]. This analysis used the original fluid activation approach, whereby material is shifted between elements of equal volume without accounting for more detailed fluid behaviour such as mixing or residence time distribution in tanks and pipes. The two water circuits used in the experiment are shown in Fig. 1: circuit #2 included a large-volume water expansion tank (WET) for neutron detection which was not present in circuit #1. For circuit #1, GammaFlow predicted gamma-ray counts in a CsI detector from ^{16}N activation with a good degree of accuracy: C/E=0.87(11) (where C/E is the ratio of calculated to experimental result). For circuit #2, in which complex fluid behaviour would be more significant, the predictions were less accurate, with C/E values approaching 0.5 at low flowrates.

In recent work published by F4E [6], the equations for radionuclide concentration have been adapted to account for WET residence time distributions in the same FNG experiments, calculated using computational fluid dynamics (CFD). The resulting correction factors significantly reduce the discrepancy between modelling and experimental observation, particularly at low flowrates. This suggests that the WET was the main source of the previous inaccuracy, and showed that including CFD in activation calculations is achievable for simple models and can make a significant difference to these C/E results.

For the current work the two CCFE fluid activation codes have been developed to include fluid dynamics and explore their capabilities, representing a first combination of these codes with CFD calculations. The FNG benchmarking analysis is continued, with effort focused on determining the source of outstanding discrepancies and achieving a first benchmark for ActiFlow. Finally, activation analysis is performed for flowing lithium-lead in a water-cooled lithium-lead (WCLL) breeder blanket test case, using material flow paths determined using CFD and comparing with simplified approaches.

2. Fluid scenarios

Two fluid scenarios – water and lithium-lead – have been evaluated in this work. These are described in the following subsections.

author's email: thomas.berry@ukaea.uk

2.1 Water activation experiments

Coolant water in future tokamaks including ITER will be activated by fusion neutrons. The most active nuclides are produced in (n,p) reactions on ^{16}O and ^{17}O isotopes [7,8]. The reaction on ^{16}O produces ^{16}N. This decays via beta decay, with a half-life of 7.13 s, and subsequent gamma-ray emission occurs at energies of 6.13 MeV (I=67%) and 7.12 MeV (I=5%) [9]. This will generate increased activity outside the biological shield and is important for safety, for heating in cryogenic systems and for dose to electronics. The reaction on ^{17}O leads to neutron and gamma-ray emission which at the ITER scale could be enough to cause non-negligible secondary activation of pipes and equipment [7,8]. In the present work only the reaction on ^{16}O is evaluated, so all results are given in terms of measured and calculated gamma-ray detection rates.

$$^{16}O\ (n, p)\ ^{16}N \rightarrow\ ^{16}N\ (\beta\ (7.13\ s)) \rightarrow\ ^{16}O + \gamma$$

Water in the circuit (Fig. 1) passed through an ITER first-wall (FW) mock-up where it was irradiated by the FNG neutron source. The water then flowed through the neutron detection (JCC-15) WET (circuit #2 only), the gamma-ray detection (CsI) WET, and a delay tank to ensure the decay of all water before being sent back to the mock-up to complete the circuit.

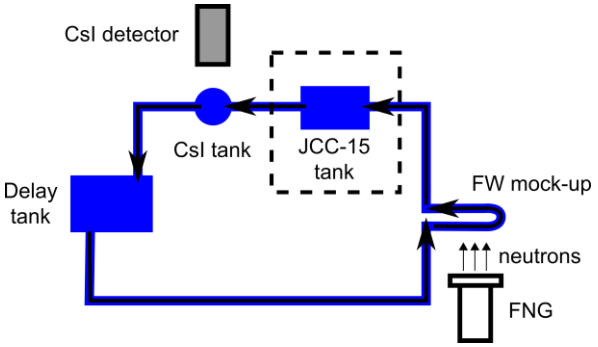

Figure 1. Schematic of the FNG water activation circuit [5], with arrows showing water flow. Circuit #1 excluded the JCC-15 tank. Circuit #2 included all tanks as shown.

The experiments were performed for a range of water flow rates, between roughly 10 $Lmin^{-1}$ and 55 $Lmin^{-1}$, and were repeated for two different distances between the FNG source and mock-up (2 cm and 5 cm). All results in this work use a source separation of 5 cm.

2.2 Flowing lithium-lead breeder material

The tritium breeder blanket is key to achieving the conditions for tritium fuel self-sufficiency in future tokamaks. The WCLL design is one of two European designs being considered for the ITER test blanket modules (TBMs) and the EU-DEMO blanket modules [10]. The molten lithium-lead in the WCLL model cycles through the blanket modules throughout operation. It therefore experiences a changing neutron flux over time. Understanding the decay heat and activity of the breeder material is important to loss-of-coolant accidents (LOCA), waste disposal and decommissioning. Previous published decay heat analysis has not taken the flowing nature of this material into account [11].

Preliminary blanket calculations in ActiFlow have assumed a single linear path through the lithium-lead manifold, around a breeder zone loop and back through the manifold. For each leg of the circuit, a single lithium-lead flow speed was assumed: 13 mm/s through the manifold; 0.25 mm/s in the feed and return legs of the breeder zone loop; and 0.10 mm/s crossing the front of the breeder zone. However, laminar flow in the channels would be expected to create a distribution in travel times through the high-flux region.

3. Code descriptions and capabilities

3.1 ActiFlow

ActiFlow solves problems using a mesh-based approach. As an input it takes an MCNP [12] output neutron flux mesh file. A mesh-based approach removes the need for an exact definition of the flow volume. ActiFlow takes a user-input coordinate flow path and flow speeds, plotting this path through the neutron flux mesh (or adjacent meshes). The path is split by the voxels it passes through. The time spent in each voxel and the flux in that voxel are calculated and stored in a list. As well as the user-defined path through the geometry, a zero-flux pseudo-voxel can be added to represent a given fraction of time spent outside the flux mesh. Multiple flow paths can be defined in the same input, in order to simulate splitting and recombination of the flow or distributions in flow speed through the same section of the circuit. These are treated independently by the code, with no in-cycle splitting or mixing, but may be combined in post-analysis.

Using FISPACT-II, the code cycles a mass unit (1 kg) of the user-defined material through the list of voxels consecutively, performing an activation calculation for each and passing the output inventory for a voxel as an input for the next voxel. A full cycle is calculated individually starting and ending on each voxel, to give a final inventory for every voxel in the cycle. .

To calculate the gamma-ray count rate for the water activation experiment, the code uses the isotope concentrations in the voxels in the detector region alongside calculated efficiencies for the ^{16}N decays [4]. To calculate the decay heat across a circuit, the decay heat (kW/kg) is averaged across the voxels in the path, weighting by the time spent in each voxel. This accounts for variation in flow speed resulting from variation in channel cross-section, and corrects the material volume accordingly. For multiple-path CFD calculations, the same voxel average is made for each path, and then the average of all paths is taken.

3.2 GammaFlow

GammaFlow uses a cell-based approach, taking calculated neutron reaction rates (here from MCNP)

inside fluid cells and using these, along with known decay half-lives, to calculate the rate of decay in given tanks in the circuit. This is converted to an observed gamma-ray detection rate with additional information on the gamma-ray branching and detection efficiency.

GammaFlow provides the user with an API with which they can build a model in which cells and circuit components are joined by pipe elements with specified volumes. Material is moved around the circuit in a cycle. The circuit is divided by the code into cells of generally equal volume, simplifying the movement as material can be assumed to transfer entirely to the next cell. This also allows for path splitting and in-cycle mixing, as the movement is time-stepped and so the cells are synchronised in time. Where adjacent cells are not of equal volume, a fraction is transferred assuming constant volumetric flow.

4. Calculations and results

4.1 Computational fluid dynamics

Previously, calculations in GammaFlow and ActiFlow have assumed a uniform velocity profile, with residence times in large components proportional to the volume. Due to the flatter profile and mixing through eddy transport, these assumptions hold well for turbulent pipe flow, but in other cases a uniform velocity profile is not appropriate.

In pipes or duct sections where the flow is laminar, faster flow in the middle of the channel leads to a distribution in residence times. One example of laminar flow in a fusion component is a lithium-lead blanket where low rates of flow lead to a sufficiently low Reynolds number for the flow to remain laminar (Re<2000 [13]). Additionally, in expansion tanks turbulence may lead to a spread in residence times. This could include residence tanks in coolant water circuits.

To examine large-volume and complex-shaped components, the residence time was calculated for different flow trajectories using the simpleFoam solver from OpenFOAM 7 [14] for the CsI WET and JCC-15 WET (shown in Fig. 2). The geometries were meshed with snappyHexMesh to yield an average dimensionless wall distance, y_1^+, of 30 to ensure valid use of wall functions with the realisable k-epsilon turbulence model. The total mesh cell counts were 10 million for the CsI expansion tank and 1.1 million for the neutron tank. The residence time calculation was done by solving the steady state flow and measuring the integration times for streamlines from the inlet to the outlet in Paraview. A distribution of residence times was found depending on the seed point and subsequent path of the streamline, which were in general shorter than the residence time calculated based on flow speed and volume. This work shows that there are geometrical fluid dynamics effects in large-volume and complex-shaped components that may need accounting for in a fluid activation code.

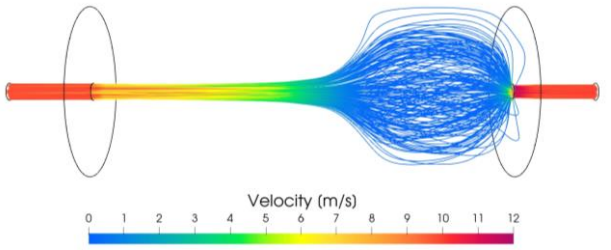

Figure 2. OpenFOAM-calculated velocity streamlines through JCC-15 WET at a flow rate of 55.1 L/min.

4.2 Water activation benchmarking

4.2.1 Pipe CFD in GammaFlow

The GammaFlow code model of FNG circuit #1 was extended to include a radial velocity profile generated using the OpenFOAM CFD. The CFD model simulated water flow through an approximated FW mock-up and the first part of the pipe (length 17.4 m, diameter 11 mm) leading from the mock-up outlet to the CsI WET. The velocity profile provided pointwise data for the velocity of the water across the diameter of the pipe leaving the mock-up. This allowed the pipe within the GammaFlow model to be split into 20 discrete radial channels, for which no mixing between these channels was assumed.

The results, shown in Fig. 3, suggest that a radial velocity profile in the pipes can have a noticeable effect on measured activity, with greater difference (of up to 9%) observed at lower flowrates where the Reynolds number is lower. This could be relevant to reactor coolant water circuits containing long, thin pipes. The results appear to account for some of the approximate 10% difference between calculation and measurement for this experiment [4], but not at higher flowrates. Furthermore, any turbulence as would be expected in such a pipe would reduce the size of the correction. The calculation demonstrates that GammaFlow can be used where there are multiple flow speeds along the same path.

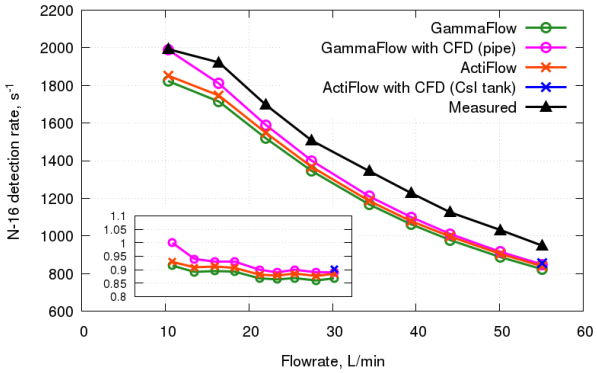

Figure 3. Measured and calculated ^{16}N activity in CsI tank for FNG circuit #1 using GammaFlow and ActiFlow, with and without fluid dynamics considerations. Inset: C/E values are plotted for calculations.

4.2.2 Expansion tank CFD in ActiFlow

Linear path inputs to ActiFlow were created for both FNG circuits. Flow speeds in each component were calculated using the volume and flow rate. CFD residence times were then calculated for the CsI WET (circuit #1) and the JCC-15 WET (circuit #2) separately. These residence time distributions were sorted into between nine and twelve bins, with each bin used to define a separate path in the ActiFlow input. For comparison, the CFD residence times calculated for the JCC-15 WET in separate work by F4E (ref. [6]) were used to create another set of inputs.

The results were compared with the original (no CFD) GammaFlow results (ref. [4]) and those measured in the experiment. The gamma-ray emission in ActiFlow was obtained using the number of ^{16}N atoms in the CsI WET, inlet and outlet, as calculated by FISPACT-II, the known half-life (Section 2.1), and the detection efficiency of 2.32% in the energy range 5.5–6.5 MeV, calculated previously by MCNP simulation [4]. This is equivalent to the approach used for GammaFlow.

The results of the circuit #1 analysis are shown in Fig. 3. ActiFlow predicts virtually the same count rates as GammaFlow, with an average accuracy of C/E=0.90(2). Summing the neutron fluence experienced by the material on the two paths through the FW mock-up (using cells in GammaFlow and mesh tally voxels in ActiFlow), the ActiFlow material sees almost identical fluence to that in GammaFlow. The calculation demonstrates that for a basic water circuit ActiFlow and GammaFlow give similar results, here predicting ^{16}N count rates within 2% of each other at all flow speeds.

The remaining 5–15% underestimation is suggested to result from fluid behaviour. Residence times were calculated for the CsI WET using the CFD approach described in Section 4.2, for one flowrate (55.1 L/min, see Fig. 3). The difference between the ActiFlow results with and without CFD is small, suggesting that the CsI WET is not the dominant source of the underestimation for circuit #1. However, water flow through the FW mock-up and pipes could explain the difference.

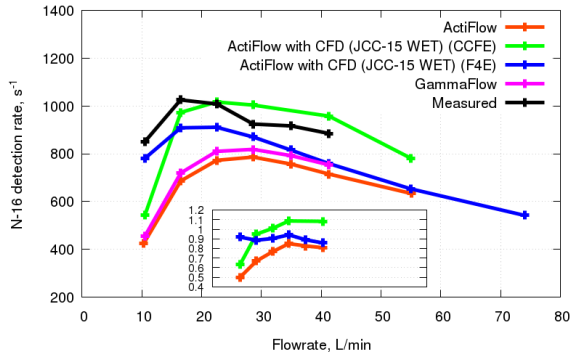

Figure 4. Measured, ActiFlow (with and without JCC-15 WET CFD residence times) and GammaFlow activity in FNG circuit #2. GammaFlow results are identical to those calculated in ref. [4]. Inset: C/E values for calculations.

The underestimation is more exaggerated for circuit #2 where, for ActiFlow and GammaFlow without CFD, at low flowrates in particular the C/E values are as low as 0.5 (Fig. 4). The flowrate dependence is consistent with the omission of fluid dynamics behaviour in the neutron tank. This is discussed in refs. [4,6]. The results for both circuits demonstrate that ActiFlow and GammaFlow give similar results when CFD is not included.

The ActiFlow results incorporating CFD in the JCC-15 WET differ depending on the source of the residence times (CCFE or F4E). When the residence times calculated by CCFE are used, the underestimation at the lowest flowrate reduces to 36% while at the highest measured flowrate ActiFlow overestimates the count rate by 8%, with a root-mean-square deviation (RMSD) from unity of 0.172. If instead the residence times calculated by F4E are used, the underestimation at the lowest flowrate is just 8%, and at the highest measured flowrate the underestimation is 14%, with a RMSD of 0.104. We suggest that the inclusion of a longer (hence more accurate) WET inlet pipe in the F4E simulation increases jetting at low flowrates, leading to higher count rates. A difference of selected turbulence model may also account for some of the difference. This highlights the importance of accurate conditions and the value of comparing simulations.

Table 1. Calculated and measured ^{16}N counts per second (CPS) by flow rate for both FNG water activation circuits, at a source-FW distance of 5 cm.

Flow rate, L/min	Circuit #1 ^{16}N count rate, CPS					Flow rate, L/min	Circuit #2 ^{16}N count rate, CPS			
	GammaFlow	GammaFlow with pipes CFD	ActiFlow	ActiFlow with CsI tank CFD	Measured		ActiFlow	ActiFlow with CCFE CFD†	ActiFlow with F4E CFD‡	Measured
10.3	1824	1985	1852	–	1993	10.5	424	543	781	852
16.4	1714	1806	1746	–	1922	16.5	686	973	908	1025
22.0	1519	1585	1548	–	1697	22.5	773	1017	911	1008
27.5	1345	1398	1367	–	1507	28.6	786	1004	870	924
34.4	1167	1208	1186	–	1344	34.9	757	–	816	917
39.4	1062	1097	1079	–	1228	41.3	715	957	759	885
44.1	978	1009	996	–	1125	55.0	–	781	653	–
50.1	887	915	904	–	1031	74.0	–	–	542	–
55.1	823	848	839	855	948					

†CFD calculations for JCC-15 WET performed by CCFE. ‡CFD calculations for JCC-15 WET performed by F4E in separate work presented in ref. [6].

4.3 ActiFlow calculations with a PbLi test case

A breeder zone test case was devised in order to examine the effect of CFD inclusion for lithium-lead flow (without magnetohydrodynamic effects). This was a single loop through a DEMO WCLL blanket consisting of homogenised layers (mixtures of tungsten, Eurofer, water and lithium-lead). The lithium-lead corresponds to a $Pb_{83}Li_{17}$ mixture containing 17.5% lithium. The loop was in the outboard equatorial plane (Fig. 5), moving from an inlet surface, along a feed channel radially towards the first wall, up and around a buffer plate, and along a return channel to the outlet surface. The model used a simplified Cartesian blanket geometry and a planar source created using the flux in front of the first wall in the DEMO model as described below.

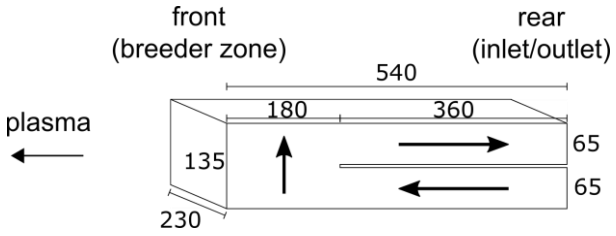

Figure 5. Dimensions of lithium-lead DEMO WCLL breeder zone test case (mm). Arrows show PbLi flow direction.

A CFD calculation was performed using liquid lithium-lead, and flow paths and speeds were calculated for tracks beginning on the inlet and ending on the outlet. Between reaching the outlet and re-joining at the inlet, a zero-flux time of 67% of the total cycling time, representing manifold and ex-blanket time, was added. The neutron flux was calculated in MCNP 6.2 with nuclear transport data from JEFF 3.3 [15]. This used the 2017 DEMO baseline MCNP model. The ActiFlow calculation used the 5.2-year DEMO phase 1 (20 displacements per atom (DPA)) irradiation schedule. EAF-2010 [16] was used for activation and decay data. The lithium-lead was cycled in ActiFlow with an averaged flux throughout the schedule and the exact breeder zone path was only used in the final circuit. Five path scenarios were simulated:

(i) a simple non-CFD square loop with path down the centre of channels and speeds as described in Section 2.2;

(ii) identical to (i) but travelling to the front of the breeder zone, representing a conservative case;

(iii) one flow path, using a CFD track beginning in the centre of the inlet surface;

(iv) four flow paths, using CFD tracks beginning at points forming a uniform 2x2 grid on the inlet surface;

(v) 25 flow paths, using CFD tracks beginning at points forming a uniform 5x5 grid on the inlet surface.

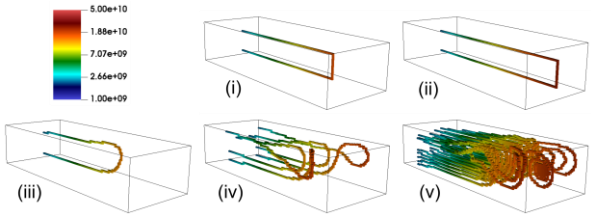

Figure 6. Neutron fluxes (n/cm^2/s) through voxels of the five different PbLi test case flow simulations.

The plots in Fig. 6 give an indicator of the flow paths and neutron fluxes in each of the calculations. The post-irradiation decay heat (kW/kg) for each test case was obtained using the path averaging method in Section 3.1. The results are shown in Fig. 7.

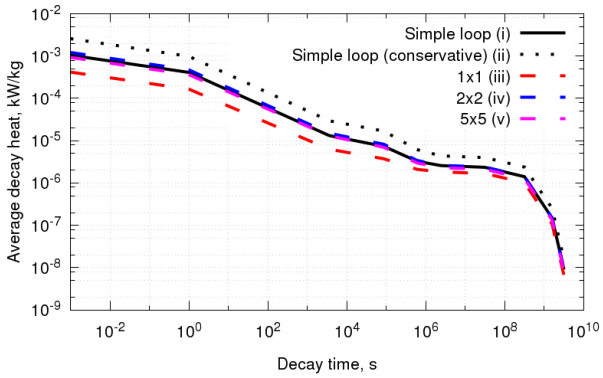

Figure 7. Decay heat per unit PbLi for different CFD and non-CFD flow path scenarios (described in text) through the breeder zone test case shown in Fig. 5.

The differences in decay heat are greater at short timescales. At shutdown, relative to the result of 1.05×10^{-3} kWkg^{-1} for the simple loop (i) calculation, the conservative loop is 152% hotter, the 1x1 loop is 56% cooler, the 2x2 loop is 28% hotter and the 5x5 loop is 9% cooler. After one year, relative to 2.35×10^{-6} kWkg^{-1} for the simple loop (i), the conservative loop is 69% hotter, the 1x1 loop is 28% cooler, the 2x2 loop is 1% hotter and the 5x5 loop is 11% cooler. The results indicate that a more detailed description of the flow through the breeder zone has a significant effect on the predicted blanket activation, with the most detailed and physically accurate flow (v) giving less conservative estimates than the simple loop (i). When using CFD, a single streamline (iii) passes tightly around the baffle plate and appears unsuitable to represent the whole flow. Using four streamlines (iv) samples more of the breeder zone but gives higher decay heat estimates than (v), with increased uncertainty owing to the small number of points sampled. A simplified path down the centre of the channel gives results reasonably close to a calculation using a number of streamlines, and so is a fair assumption where complete accuracy is not essential.

5 Discussion and conclusions

Both GammaFlow and ActiFlow have now been compared with experimental water activation results. By

accounting for CFD in the WET in ActiFlow calculations for circuit #2, the outstanding discrepancy is now around 10% across most flowrates for both circuits, although this depends on the approach taken. It is possible that accounting for radial velocity distributions in the pipes could provide a further correction at low flowrates only, but further work is needed. The remaining difference is therefore expected to result from residence time distributions inside the FW mock-up component.

Through this work the strengths and weaknesses of the two codes have been clarified and the impact of considering fluid behaviour in activation calculations has been highlighted. The strengths of the GammaFlow code lie in its ability to accurately model a spatially well-defined flow in a relatively fast calculation time, for simple materials. It is well-suited to modelling coolant water circuits, where pipe networks contain points where many pipes split and re-join. ActiFlow is versatile in terms of the materials, reactions and paths which it can model. The multiple-flow capability allows the code to account for residence time distributions or path splitting in limited situations. The mesh-based approach is inefficient when simulating well-defined flows such as the FNG water activation circuit, but advantageous where flow geometry is not completely defined. In addition, as demonstrated through the PbLi test case study it allows for more detailed analysis of individual flow paths.

Within a reactor environment, pipe systems can often take the form of lengthy and complex networks including components such as junctions, holding tanks and pumps. Due to the complex nature of these systems, the computational cost of full-system CFD calculations could be prohibitive. One way to overcome this could be to create a repository of common components where each could be modelled using a CFD code, generating a radial velocity profile. Users could then build a model with these parametrised components using the GammaFlow API, allowing fast, standardised calculations which account for fluid dynamics throughout the system.

The two codes have advantages and disadvantages owing to different approaches, and between them cover a range of problems. A combined code would therefore be advantageous, with the possibility of choices between mesh-based and cell-based sampling, the use of known reaction/decay parameters or an activation code, and user-defined cells or parametrised components.

Acknowledgments

Part of this work has been carried out within the framework of the EUROfusion Consortium and has received funding from the Euratom research and training programme 2014-2018 and 2019-2020 under grant agreement No633053. The views and opinions expressed herein do not necessarily reflect those of the European Commission. Part of this work has been carried out with funding from Fusion for Energy (F4E) contract number F4E-OPE-0956. Part of this work has been carried out with funding from EPSRC Grant EP/T012250/1.

References

[1] A. Žohar and L. Snoj, Prog. Nucl. Energy **117**, 103042 (2019).

[2] I. Palermo *et al.*, Fusion Eng. Des. **153**, 111499 (2020).

[3] J.-Ch. Sublet *et al.*, NDS **139**, 77 (2017).

[4] C. R. Nobs *et al.*, Fusion Eng. Des. **159**, 111743 (2020).

[5] F. Andreoli *et al.*, EPJ Web Conf. **239**, 21002 (2020).

[6] R. Pampin *et al.*, Nucl. Fusion **61**, 036002 (2021).

[7] V. Khripunov and R.T. Santoro, *Radionuclide Production in the ITER Water Coolant*, ITER Report No. G30 RI 1 (1996).

[8] Q. Yang *et al.*, Fusion Eng. Des. **87**, 1310 (2012).

[9] D. R. Tilley, H. R. Weller and C. M. Cheves, Nucl. Phys. A **564**, 1 (1993).

[10] J. Aubert *et al.*, Fusion Eng. Des. **160**, 111921 (2020).

[11] T. Eade *et al.*, Fusion Eng. Des. **124**, 1241 (2017).

[12] D. B. Pelowitz, *MCNP6 User's Manual Version 1.0*, LANL Report LA-CFP-13-00634 (2013).

[13] O. Reynolds, Philos. Trans. R. Soc. **186**, 123 (1895).

[14] H. G. Weller *et al.*, Comput. Phys. **12**, 620 (1998).

[15] A. J. M. Plompen *et al.*, Eur. Phys. J. A **56**, 181 (2020).

[16] J.-Ch. Sublet *et al.*, *The European Activation File: EAF-2010 neutron-induced cross section library*, CCFE-R (10) 05 (2010).